Original Research

Divergent Neural Processes Specific to the Acute and Sustained Phases of Verum and Sham Acupuncture

Jixin Liu, PhD,[1] Wei Qin, PhD,[1] Qian Guo, MS,[1] Jinbo Sun, PhD,[1] Kai Yuan, PhD,[1] Minghao Dong, PhD,[1] Peng Liu, PhD,[1] Yi Zhang, PhD,[1] Karen M. von Deneen, MD,[3] Yijun Liu, PhD,[3] and Jie Tian, PhD[1,2*]

Purpose: To discuss which brain region potentially functioned and switched between the immediate and delayed response of acupuncture.

Materials and Methods: A nonrepeated event-related functional MRI (fMRI) design was used to investigate the spatial and temporal patterns of acupuncture effects induced by needling an acupoint ST36 (ACU) and a nonmeridian point (SHAM). The standard general linear model was used to detect the immediate neural responses of acupuncture. Graph theory analysis was used to characterize the functional integrated network of the acupuncture delayed effect.

Results: Acupuncture induced significant signal changes in the limbic/paralimbic areas, neocortical regions, brainstem, and cerebellum for immediate effect both in ACU and SHAM. Some of these brain regions showed strong functional connectivity for a delayed effect in ACU. Conjunction analysis showed that the insula played a critical role during the overall process of ACU. No overlapping brain regions were found in SHAM.

Conclusion: The findings of this study suggested that the delayed effects may reflect a more significant characteristic underlying acupuncture. Given that the insula as a relay station switched between the immediate and delayed response, it suggested that divergent functional connectivity patterns may mediate the acupuncture-related effects for ACU and SHAM.

Key Words: acupuncture; immediate response; delayed effect; graph theory analysis
J. Magn. Reson. Imaging 2011;33:33–40.

ACUPUNCTURE HAS SERVED as a clinical treatment for various illnesses for thousands of years (1). It is used widely for several disorders such as agitation, depression, stress, poststroke paralysis, facial palsy, and epilepsy (1). However, physiological mechanisms and neural pathways underlying acupuncture effects are still not well understood. It has long been acknowledged that the whole process of acupuncture is composed of two main parts: the acute phase and sustained phase (Fig. 1B). The acute phase initially probes the spatial distribution of acupuncture-induced brain regions, and the sustained phase focuses on the temporal pattern of the dynamics for the acupuncture-related brain activities (2–7).

Previous acupuncture studies using functional MRI (fMRI) methods, under the "on–off" design paradigm, focused on the acute effects of acupuncture, i.e., the immediate response to manipulation of acupuncture, rather than the delayed effects (8–10). This design is based on the assumption that the effect of the stimulus during the "on" period will have little effects during the "off" period, such as blood oxygenation level-dependent (BOLD) signal changes for most perceptual or cognitive stimuli (11). Most acupuncture studies used the "on–off" design paradigm detecting regional brain activity in response to the needle stimulus (8,10). Most of these studies have typically identified an attenuation or modulation of the BOLD signal in the limbic/paralimbic, brainstem, and neocortical regions (8,9). However, evidence from acupuncture analgesia studies suggested that a delayed response existed during the resting state following acupuncture stimulation (12). Recent controversy in acupuncture research was generated when the "on–off" design protocol was separated into different conditions across each subject, evaluating the difference between the baseline and the subsequent epochs. It showed that the activity pattern during the postacupuncture resting epoch was prominently associated with stimulus-related

[1]Life Sciences Research Center, School of Life Sciences and Technology, Xidian University, Xi'an, Shaanxi, China.
[2]Institute of Automation, Chinese Academy of Sciences, Beijing, China.
[3]Departments of Psychiatry and Neuroscience, McKnight Brain Institute, University of Florida, Gainesville, Florida, USA.

Contract grant sponsor: National Natural Science Foundation of China; Contract grant numbers: 81000641, 81000640, 81071217, 81001504, 31028010, 30970774, 60901064, 30930112, 30901900, 30873462 and 30870685; Contract grant sponsor: Chinese Academy of Sciences; Contract grant number: KGCX2-YW-129; Contract grant sponsor: Project for the National Key Basic Research and Development Program (973); Contract grant numbers: (973) 2006CB705700 (863) 2008AA01Z411; Contract grant sponsor: Fundamental Research Funds for the Central Universities.

*Address reprint requests to: J.T., Life Sciences Research Center, School of Life Sciences and Technology, Xidian University, Xi'an 710071, China. E-mail: tian@ieee.org

Received May 6, 2010; Accepted September 13, 2010.
DOI 10.1002/jmri.22393
View this article online at wileyonlinelibrary.com.

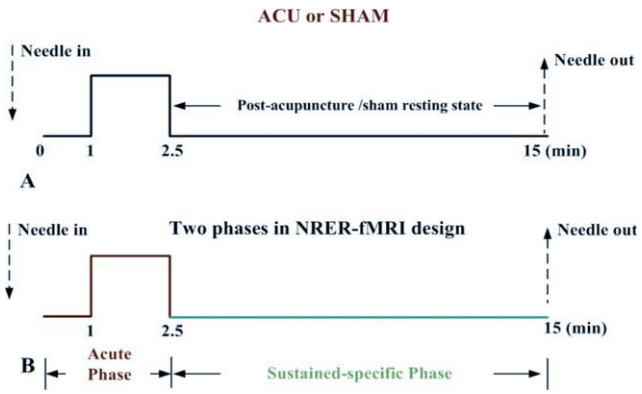

Figure 1. Experimental paradigm. **A:** The NRER design run lasted 15 min. **B:** Acute phase and sustained phase.

effects (13,14). These results provided direct evidence for the sustained central effect of acupuncture, and indicated that the precise timing and duration of the acupuncture effect cannot be specified a priori. Furthermore, Liu et al and Bai et al pointed out that the influence of the sustained effect of acupuncture may lead to statistical significance errors if the "on–off" experimental paradigms were used (8,9), which has unfortunately been ignored in most acupuncture studies.

Recently, researchers have shown an increased interest in the sustained effects of acupuncture (2–7,13–15). Bai et al pointed out that the delayed response of the acupuncture effect varied with acupoints in the sustained phase, which was presented as distinctive patterns with time (4). Moreover, many studies reported that acupoint specificity studies should not only concern the immediate effect of acupuncture, but also pay attention to the delayed effect of the acupuncture-induced neural response (2,4–6). More recently, Qin et al used the nonrepeated event-related fMRI (NRER-fMRI, Fig. 1A) design to investigate delayed responses after acupuncture administration (3,15). As compared with the "on–off" design paradigm, this one has the advantage of considering the spatial and temporal information respectively in the whole process of acupuncture. Considering the long-lasting effects of acupuncture, the NRER-fMRI design may help to define its specific mechanisms underlying the acupuncture-brain interaction.

Based on the NRER-fMRI experimental paradigm, our study aimed to designate the characteristics of acute and sustained phases, and investigate the spatial and temporal patterns of brain responses modulated by acupuncture stimulation. In this article, we assessed brain activities induced by acupuncture stimulation at an acupoint ST36 (ACU) and a nonmeridian point (SHAM) to explore how the neural responses were altered during the acute phase. We also investigated the functional connectivity intensity of acupuncture-induced brain regions to detect whether brain responses exhibited distinct patterns after acupuncture during the sustained phase. This analysis could address the lack of differentiation between ACU and SHAM. More importantly, the neural substrate underlying acupuncture would be characterized more comprehensively.

In our current study, neural responses during the acute phase of acupuncture were based on the typical general linear model (GLM) contrast analysis. Graph theory analysis (GTA) was used to characterize the functional integrated network of sustained responses induced by acupuncture during the sustained phase. GTA has the advantages of evaluating the strength as well as the temporal and spatial patterns of interactions in the human brain (16), though by defining a graph as a set of nodes (brain regions) and edges (functional connections). This approach has successfully been applied in many previous brain network studies (5,17–19). Liu et al previously applied GTA to characterize the development of brain networks for the sustained effects of acupuncture over time, but were limited to a set of 63 predefined brain regions (5). Thus, it may not comprehensively describe the characteristics of the acupuncture network. In this study, we extended GTA to high-resolution mapping and whole brain analysis. Accordingly, we could fully characterize the prominent status and contribute the continuous basis related to acupuncture.

MATERIALS AND METHODS

Subjects

Fourteen right-handed college students were recruited (7 males and 7 females, 21.4 ± 1.3 [mean ± SD] years old). The subjects were acupuncture naive and did not have a history of major medical illnesses, head trauma, neuropsychiatric disorders, had not used prescription medications within the last month, and had no contraindications for exposure to a high magnetic field. All subjects were given written, informed consent after the experimental procedure had been fully explained, and all research procedures were approved by a local Subcommittee on Human Studies and were conducted in accordance with the Declaration of Helsinki.

Experimental Procedures

Each subject participated in two fMRI scanning sessions. The interval between sessions was 7 days to eliminate potential long-lasting effects after acupuncture administration. Session 1 and 2 were both acupuncture experiments (a manual acupuncture condition, ACU; a sham acupuncture condition, SHAM). The type and order of stimulation were blinded to all subjects. During the procedure, subjects were required to keep their eyes closed to prevent them from actually observing the procedures. The sequence of ACU and SHAM protocols was randomized across all fMRI runs, and the order of presentation was counterbalanced across subjects. Acupuncture was performed at acupoint ST36 (Zusanli, located four finger breadths below the lower margin of the patella and one finger breadth laterally from the anterior crest of the tibia) on the right leg. This is one of the most frequently used acupoints and proven to have clinical effects in the treatments of

gastric and intestinal diseases, and pain-management in both humans and animals (4,20). Acupuncture stimulation was delivered using a sterile disposable 38 gauge stainless steel acupuncture needle, 0.2 mm in diameter and 40 mm in length. The needle was inserted perpendicularly to a depth of 2–3 cm. The acupuncturist then rotated the needle clockwise and counterclockwise for 1 min at a rate of 60 times per min. The same experienced and licensed acupuncturist participated in the whole experiment.

In this study, we used the NRER-fMRI experimental design, and only a single stimulation period was performed in each of these two runs (Fig. 1A). In ACU, an acupuncture needle was inserted at ST 36 for 1 min without manipulation and then the needle was manipulated for 1.5 min (Fig. 1A); the needle remained in the acupoint for another 12.5 min. In SHAM, the procedure was the same as in ACU except that the stimulation was administered at a nonacupoint (2–3 cm apart from ST 36).

Psychophysical Data Collection and Analysis

At the end of each fMRI scan, subjects were asked to quantify their sensations using a 10-point visual analogue scale (VAS). The sensations are all listed on the MGH acupuncture sensation scale (MASS), including aching, pressure, soreness, heaviness, fullness, warmth, coolness, numbness, tingling, and dull or sharp pain and one blank slot for subjects to add their own words if the above descriptors did not embody the sensations they experienced during stimulation (21). A different data interval of VAS represented the various extent of the sensations of the subjects, where 0 = no sensation, 1–3 = mild, 4–6 = moderate, 7–8 = strong, 9 = serve and 10 = unbearable sensation. Because sharp pain was considered an inadvertent noxious stimulation (8), the subject whose scale feeling of sharp pain greater than the mean by more than two standard deviations was excluded from further analysis. No subject added an additional descriptor in the blank slot provided.

Imaging Data Acquisition and Analysis

The experiment was carried out in a 3 Tesla (T) GE scanner using a standard GE whole head coil (LX platform, gradients 40 mT/m, 150 T/m/s, GE Medical Systems, Milwaukee, WI). A custom-built head holder was used to prevent head movements. A gradient echo T2*-weighted sequence with in-plane resolution of 3.75 mm × 3.75 mm (echo time [TE] 30 ms, repetition time [TR] 1.5 s, matrix 64 × 64, field of view [FOV] 240 mm, flip angle 90°) and a set of T1-weighted high-resolution structural images were acquired (TE 3.39 ms, TR 2.7 s, matrix 256 × 256, FOV 256 mm, flip angle 7°, in-plane resolution 1 mm × 1 mm, slice thickness 1 mm).

Preprocessing

Image preprocessing was carried out using SPM5 (http://www.fil.ion.ucl.ac.uk/spm). The first 100 time points (single BLOCK) including the needle stimulus were recruited to localize the neural response resulting from acupuncture during the acute phase. Data preprocessing steps included the following: rigid body correction for geometrical displacements caused by head movement; co-registration with the Montreal Neurological Institute (MNI) EPI template image; and image smoothing with a 6mm Gaussian kernel to decrease spatial noise. The standard GLM was then used.

For the post-ACU/SHAM resting scan and resting fMRI scan, all functional images were processed using the following steps: (i) compensation of systematic, slice-dependent time shifts, (ii) elimination of systematic odd-even slice intensity differences due to interleaved acquisition, (iii) rigid body correction for geometrical displacements caused by head movement, and (iv) coregistration with the MNI echoplanar imaging (EPI) template image and resampling to 2-mm isotropic voxels.

Graph Theory Analysis

A key issue in characterizing the brain topological network is the construction of the functional connection matrix. To address this issue, we down sampled the data to 6 mm isotropic within the whole brain. We obtained 3446 nodes of interest covering the entire brain. To correct physiological noise, the fMRI time series of all nodes was first filtered using a bandpass filter (0.01–0.08 Hz) to reduce the effects of low-frequency drift and high-frequency noise. Then, we removed the signal associated with white matter, cerebrospinal fluid, six motion parameters, and the whole brain. This regression procedure can be used to remove fluctuations unlikely to be involved in specific regional correlations. We chose a relatively strict threshold for our network analysis. Finally, a 3446 × 3446 matrix of Pearson correlation coefficients was calculated on the above denoised motion corrected time courses between all possible connections of node pairs.

We invested the brain's topological properties by way of binary graphs in which each correlation matrix was thresholded. A brain functional connection could be represented as an undirected edge if the correlation coefficient between two nodes achieved a correlation threshold R. A final unweighted and undirected binary graph was created. In the current study, brain networks were constructed at the threshold of R = 0.25, which was also previously used in Buckner et al (22). The conservative threshold was selected for the reason that the adjacency matrix needed to sufficiently sparse for the network metric calculation for the brain networks (17).

In GTA, the key parameters are the degree (D) which can be used as a measure of the intensity of functional connectivity. The degree of a graph is the number of edges incident to the vertex, and it is defined as the number of nodes across the brain that showed strong correlation with the target node. The brain regions showing high value of degree in the network were considered to be a cortical hub, which may play a critical role in integrating diverse informational

sources and balancing the opposing pressure to evolve segregated, specialized pathways (22).

Statistical Analysis

To investigate the cortical hubs in the post-ACU/SHAM resting state, we measured the connectivity based on the nodal degree. By the definition of degree, the node has a higher degree, meaning that it has higher intensity of functional connectivity. To analyze all node degrees in the normalized space, the node degree was projected back to the original three-dimensional (3D) brain space for each subject's network in both ACU and SHAM. In this way, node coordinates were comparable across subjects. Counting the occurrence of the high node degree metric across subjects, we identified nodes with the top 20%node metric values. Then, the consistent patterns in the locations of the cortical hubs were obtained by averaging the image for each nodal degree metric. Finally, an overlap image would be generated, and each voxel in the image corresponded to the number of subjects with the high degree metric. Based on each nodal degree, we performed a paired t-test to determine if the degree of the brain region was significantly different between ACU and SHAM. If any changes in the topological properties were found between the two groups, we would investigate the distribution of the regions which showed significant differences in the nodal degree.

A conjunction analysis was performed to detect the statistical reliability of signal change in both the acute phase and sustained phase. Such a neural signal was contributed to the overall statistical strength, showing that the same brain regions were activated strongly and consistently in the overall process of acupuncture. This analysis aimed to detect which brain region had important function, suggesting the region's putative role in switching between the acute phase and the sustained phase.

RESULTS

Psychophysical Response

No participants reported sensing sharp pain during the entire scanning procedure. Furthermore, no significant difference was found between the sensation intensity of ACU and SHAM (paired t-test, $P > 0.05$).

Activation Sites During the Acute Phase

To detect the BOLD signal changes induced by acupuncture during the acute phase, a GLM model was calculated across each subject with regressors for the difference from baseline (BL). From the group results of the GLM statistical analysis (one-sample t-test, $P < 0.005$, uncorrected, cluster size >10 voxels as shown in Fig. 2), the average brain activations evoked during the acute phase displayed similar patterns of hemodynamic response between ACU and SHAM (Fig. 2). Group results for acupuncture at ST36 showed extensive signal changes in the limbic/paralimbic areas, neocortical regions, brainstem, and cerebellum, particularly in the insula, thalamus (THA), anterior cingulate cortex (ACC), middle cingulate cortex (MCC), bilateral substania nigra (SN), bilateral secondary somatosensory cortex (SII), anterior prefrontal cortex (aPFC), dorsolateral prefrontal cortex (dlPFC), temporal cortices, and anterior/posterior part of the cerebellum. In contrast, the BOLD response to SHAM showed positive activations with a relatively small extent of spatial distribution and less intensive signal change as compared to ST36, mainly in the insula, SII, and cerebellum. No significant change was detected in the limbic-related and brainstem regions, in contrast with the hemodynamic response to the acupuncture stimulation at ST36.

Degree Difference During the Sustained Phase

To measure the long-lasting effect of acupuncture during the sustained phase, we compared the functional connectivity network between ACU and SHAM using the following methods. We created an unweighted and undirected binary graph with a set of nodes and edges. This graph fully represented a group of functionally related brain regions from a whole brain scale (as described in the experimental procedures). For each predefined brain region, the nodal degree was calculated in both the ACU and SHAM networks. The difference in degree of each brain region could be used to detect the discrepancy of functional connectivity patterns between ACU and SHAM. Significant degree differences were found in the limbic/paralimbic regions, brainstem, prefrontal cortices, temporal cortices, and cerebellum (two-sample t-test, $P < 0.005$, uncorrected, Table 1).

Results showed that connectivity strength was higher overall in the limbic-related brain cortices in ACU than in SHAM, such as in the amygdala (AMY), parahippocampus (PH), insula, THA, and MCC (Fig. 3; Table 1). Of interest, we found a divergent connectivity pattern in the aPFC and dlPFC (Fig. 4). A higher intensity of functional connectivity was shown in the aPFC for ACU and greater connectivity strength in the dlPFC for SHAM.

Conjunction Analysis

The aim of the conjunction analysis was to explore which brain region potentially functioned and switched between the immediate and delayed response of acupuncture. By overlapping brain activations resulting from acupuncture at ST36 during the acute phase ($P < 0.005$, uncorrected) with the region having a higher degree in ACU (top 20%node degree metric ACU>-SHAM), it showed that the overlapping brain regions were mainly located in the insula and brainstem. In parallel with these findings, no significant overlapping brain areas were found in SHAM (Fig. 5).

DISCUSSION

Liu et al and Bai et al previously found that acupuncture was a slowing-acting agent and had a specific

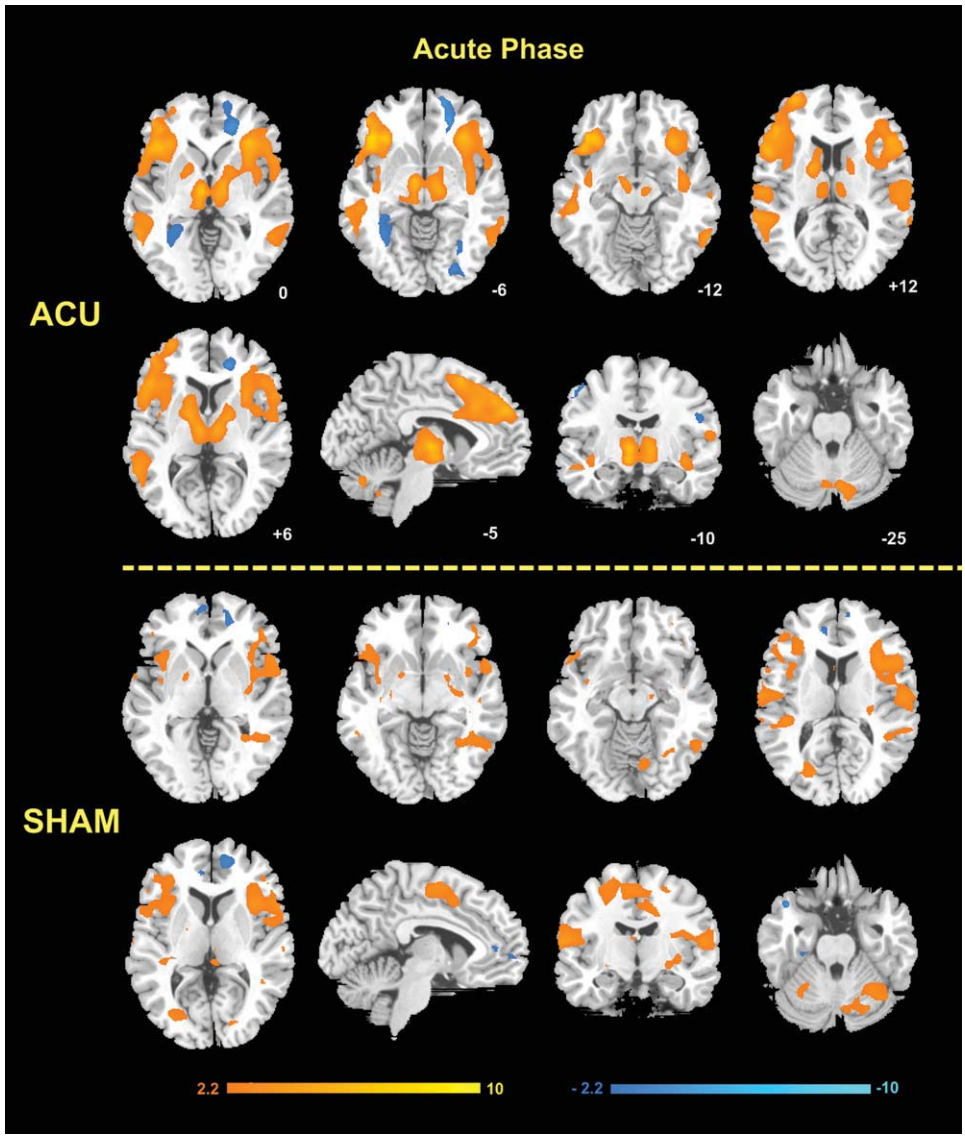

Figure 2. Group results of brain activation during the acute phase for ACU and SHAM. Statistical significance was thresholded at $P < 0.005$ (uncorrected) with a minimum cluster size of 10 voxels. Representative color-coded statistical maps under acupuncture manipulation exhibited the distribution of foci with significant increases (shown in the spectrum from orange to yellow) and decreases (shown in blue), relative to the respective baseline condition (BL).

dynamic pattern for the entire coupled nervous system (5,14). In this study, we gave a detailed description on how the acupuncture effects interact with the immediate and delayed response of acupuncture. Model based and data driven techniques were used to characterize the hemodynamic responses to the stimulation for ACU and SHAM.

Compared with SHAM, acupuncture at ST36 induced significant fMRI signal changes with a larger extent of spatial distributions during the acute phase (Fig. 2). Our results showed neural response alteration in different limbic, paralimbic, and brainstem regions (insula; ACC; MCC; THA) in ACU. However, these brain response patterns were absent in major limbic regions for SHAM (Fig. 2). Our results were consistent with previous findings (14). There was increasing evidence that revealed the significance of the acupuncture-induced neural activity of the limbic–paralimbic–neocortical networks (8,23). As we know, the limbic–cerebellar regions play a critical role in both affective and motoric pain processing (24,25), and also in the ascending pain-conductive system (14,26). In our current study, acupuncture in ACU, compared with SHAM, could evoke significantly complex neural responses during the acute phase, indicating that the immediate effect of acupuncture exhibited distinct activity patterns, particularly in the limbic system.

Meanwhile, for the delayed effects of acupuncture, some regions related to the outcome of the stimulation sensation only responded to the initial administration of acupuncture. Some brain areas that refer to the clinical effects from acupuncture treatment showed delayed responses, and continuously exerted controlling and coordinated effects throughout the scan (14). Based on our results in the sustained phase, stronger functional connectivity was found in the limbic/paralimbic areas and brainstem (AMY; PH; insula; THA; MCC) at ST36 (Fig. 3; Table 1) in ACU compared with SHAM, suggesting the limbic system may play an important role in receiving sensory information and affecting decisions and subsequent behavior (27–29).

We studied the acupuncture effect in both the acute phase and sustained phase respectively. ACU induced a relatively more intensive signal changes, and these

Table 1
Foci With Significant Changes in Degree Changes From ACU Versus SHAM During the Sustained-Specific Phase

Regions of interest		Talairach x	Talairach y	Talairach z	ACU Degree Mean ± SD	SHAM Degree Mean ± SD	*P* Value
Limbic system							
Amygdala	L	-27	-1	-15	231.6 ± 87.1	171.5 ± 78.1	0.001
	R						
Parahippocampus	L	-27	-41	-8	312.1 ± 153	171.5 ± 78.1	0.0021
	R	27	-41	-8	337 ± 139	245 ± 95.8	0.0018
Insula	L	-33	-22	18	260.8 ± 156	172.7 ± 111.1	0.0039
	R						
Thalamus	L	-9	-11	6	416.6 ± 115.4	298.7 ± 138	0.0028
	R	15	-11	6	373.3 ± 124.8	312.4 ± 140.3	0.0006
MCC BA24/31	L	-3	2	44	346 ± 95.84	243 ± 83	0.0045
	R	9	-9	45	372 ± 119.13	264 ± 130.3	0.0038
Brainstem							
Pons	L	-9	-30	-24	359.1 ± 167.5	208.8 ± 119.1	0.0007
	R	3	-13	-25	263.8 ± 108	216.6 ± 112.2	0.0041
Frontal cortex							
aPFC BA10	L	-9	47	9	357.3 ± 139.6	265.1 ± 128.3	0.0025
	R	3	59	8	305.2 ± 55.5	248.1 ± 61.7	0.0002
dlPFC BA9	L	-21	48	31	279.9 ± 58.9	337.2 ± 47	0.0003
	R						
Temporal cortex	L	-56	-69	20	106.6 ± 83.9	52.5 ± 34.9	0.004
	R	50	17	-11	348.4 ± 68.4	277.2 ± 41.5	0.003
Cerebellum							
Declive	L	-21	-59	-17	460.3 ± 115.7	375.4 ± 98.2	0.0003
	R	39	-71	-17	387.2 ± 94.5	313.5 ± 83	0.001
Culmen	L	-27	-30	-19	202.4 ± 70.6	283.1 ± 83	0.0002
	R						

signals displayed distinctive temporal patterns compared with SHAM. The conjunction analysis investigated how acupuncture interacted with internal regulatory processes, and it helped gain an appreciation of the physiological function and integrated mechanisms involved in acupuncture. In our results, the insula and brainstem were common brain regions showing greater neural activity in both phases of ACU (Fig. 5). Several acupuncture studies have already emphasized the important neural activity of the midbrain nuclei on the endogenous monoaminergic and opioidergic systems (8,30). It may suggest that the brainstem plays a critical role in the descending anti-nociceptive pathway of the central nervous system mechanism of

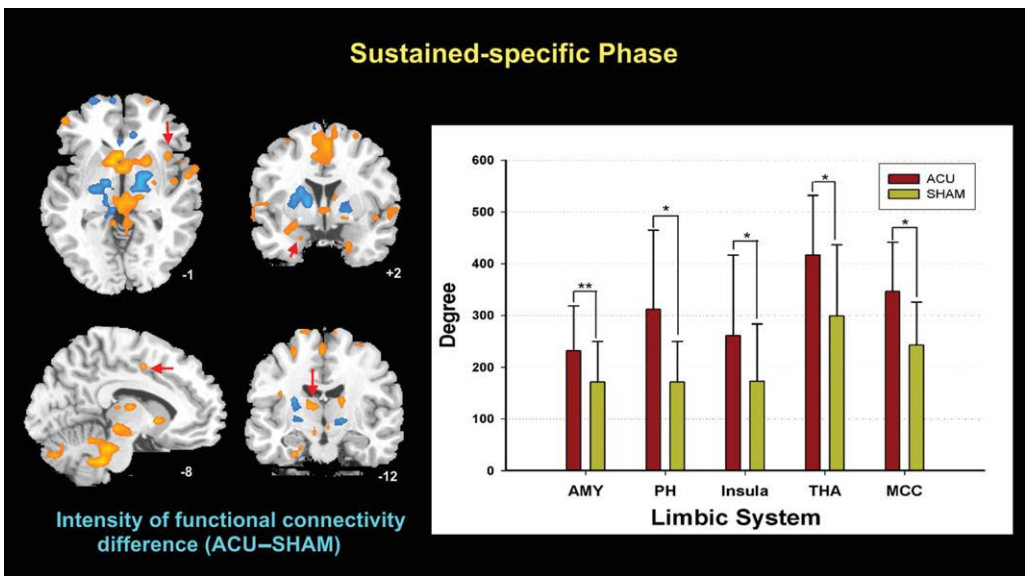

Figure 3. Group results of intensity of functional connectivity (degree) difference during the sustained phase. Significant differences in the intensity of functional connectivity in the limbic system during the sustained phase (paired t-test). Presented here are the most significant brain regions after a paired t-test. The red bars are the results from ACU, and the yellow bars are the results from SHAM. Error bars are based on a 95%confidence interval. *$P < 0.005$, **$P < 0.001$.

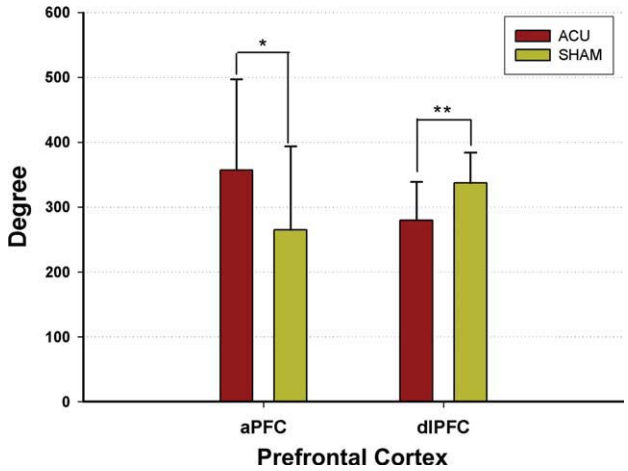

Figure 4. Significant differences in the intensity of functional connectivity (degree) in the prefrontal cortices during the sustained phase (paired t-test). The red bars are the results from ACU, and the yellow bars are the results from SHAM. Error bars are based on a 95%confidence interval. *$P < 0.005$, **$P < 0.001$.

acupuncture (5,14). On the other hand, Liu et al evaluated the development of functional connectivity along a time line during the post-ACU resting state at ST36, and found that the insula was identified as the bridge connecting the components of the brain networks following acupuncture (5). Manning and Mayer pointed out that the insula was part of the central circuitry that could mediate affective responses to pain by means of connections with the AMY and projections from the AMY to the PH (31). These results were corroborated by our results that there were prominently insula-related activations within the immediate responses and sustained effects of acupuncture. In contrast to SHAM, our results suggested that the insula was a relay station for the interoceptive awareness of both stimulus-induced and stimulus-independent changes in the acute and sustained phases, serving as a network hub to initiate dynamic switching between limbic/paralimbic areas regions. The insula integrated the centrally processed sensory information for its reciprocal connections with multiple brain regions (27,32). The insula may operate as a core brain region for monitoring the ongoing acupuncture effects.

In our results, ACU yielded different functional connectivity patterns in the prefrontal cortices during the sustained phase. Harris et al provided direct evidence of acupuncture therapy on central μ-opioid receptor (MOR) binding availability in chronic pain patients, therefore, they pointed out that it occurred by means of different MOR processes to mediate clinically relevant analgesic effects for ACU and SHAM, including the prefrontal cortices (23). Our findings were consistent with these results. For the same needling manipulation performed on the ACU and SHAM, acupuncture induced different, complex response patterns within the prefrontal cortices (Fig. 4; Table 1). Acupuncture analgesia may include cognitive mechanisms (33), and different connecting patterns in the prefrontal cortices suggesting that a divergent modulation of the brain networks may mediate the specific mechanism underlying sustained effects for ACU and SHAM.

In conclusion, our study has considered both the acute effect and sustained effect of acupuncture in a comprehensive way. Typical GLM contrast analysis and GTA were applied in the statistical analysis. The application of GTA to the acupuncture fMRI data is a

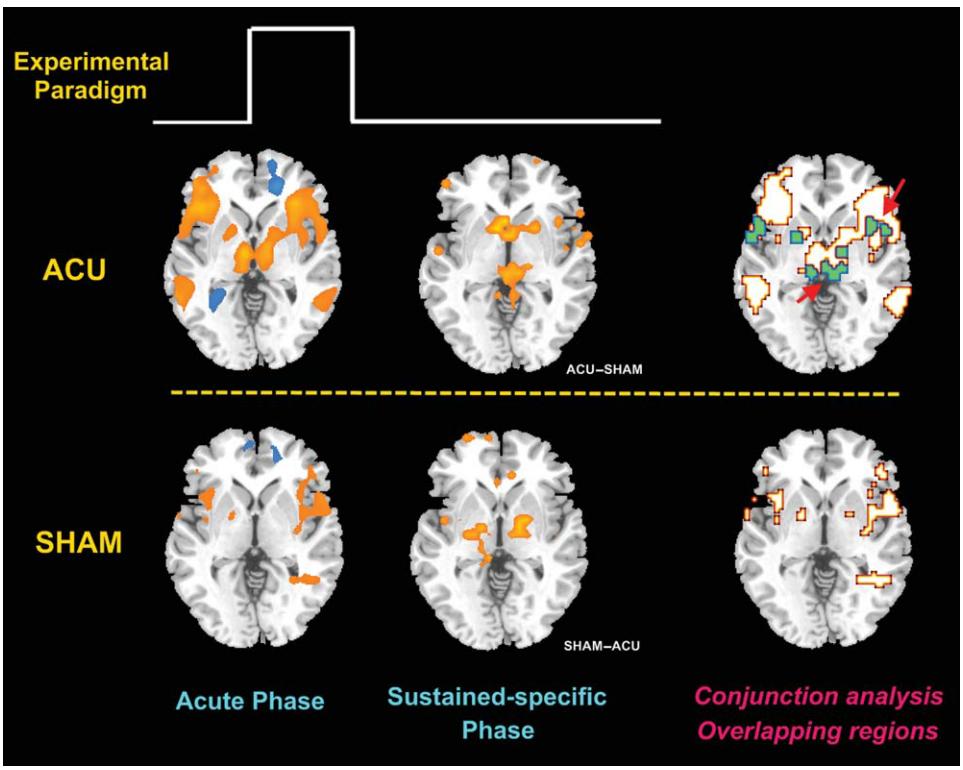

Figure 5. Conjunction analysis results. The overlapping brain regions of ACU are located in the insula and brainstem in both the acute phase and sustained phase, and no region was found in SHAM.

nascent field of research. Previously, our analysis for the sustained effects of acupuncture was limited to a set of 63 predefined brain regions (5). In our current study, we described comprehensive characteristics of the acupuncture network on a whole brain scale. Our results indicated that acupuncture at ST36 and SHAM showed similar neural responses during the acute phase, but acupuncture induced significant complex response patterns during the sustained phase in ACU. ACU and SHAM may differ in their underlying neurobiological processes, although they both may have similar peripheral inputs. The limbic system and brainstem possibly play a central role in regulating the acupuncture-induced brain regions that mediate acupuncture effects. These findings may help our future studies looking into the neural mechanisms underlying chronic pain.

ACKNOWLEDGMENTS

This study is supported by CAS Hundred Talents Program, the National Natural Science Foundation of China, the Knowledge Innovation Program of the Chinese Academy of Sciences, and the Project for the National Key Basic Research and Development Program 973 and 863.

REFERENCES

1. Ramsay DJ, Bowman MA, Greenman PE, et al. Acupuncture. NIH consensus development panel on acupuncture. J Am Med Assoc 1998;280:1518–1529.
2. Liu P, Qin W, Zhang Y, et al. Combining spatial and temporal information to explore function-guide action of acupuncture using fMRI. J Magn Reson Imaging 2009;30:41–46.
3. Qin W, Tian J, Bai L, et al. FMRI connectivity analysis of acupuncture effects on an amygdala-associated brain network. Mole Pain 2008;4:55.
4. Bai L, Qin W, Tian J, et al. Acupuncture modulates spontaneous activities in the anticorrelated resting brain networks. Brain Res 2009;1279:37–49.
5. Liu J, Qin W, Guo Q, et al. Distinct brain networks for time-varied characteristics of acupuncture. Neurosci Lett 2010;468: 353–358.
6. Zhang Y, Liang J, Qin W, et al. Comparison of visual cortical activations induced by electro-acupuncture at vision and nonvision-related acupoints. Neurosci Lett 2009;458:6–10.
7. Li L, Qin W, Bai L, Tian J. Exploring vision-related acupuncture point specificity with multivoxel pattern analysis. Magn Reson Imaging 2010;28:380–387.
8. Hui KKS, Liu J, Marina O, et al. The integrated response of the human cerebro-cerebellar and limbic systems to acupuncture stimulation at ST 36 as evidenced by fMRI. Neuroimage 2005;27: 479–496.
9. Fang J, Jin Z, Wang Y, et al. The salient characteristics of the central effects of acupuncture needling: limbic-paralimbic-neocortical network modulation. Hum Brain Mapp 2008;30:1196–1206.
10. Kong J, Kaptchuk TJ, Webb JM, et al. Functional neuroanatomical investigation of vision-related acupuncture point specificity: a multisession fMRI study. Hum Brain Mapp 2009;30:38–46.
11. Gusnard DA, Raichle ME, Raichle ME. Searching for a baseline: functional imaging and the resting human brain. Nat Rev Neurosci 2001;2:685–694.
12. Mayer DJ. Biological mechanisms of acupuncture. Prog Brain Res 2000;122:457–477.
13. Zhang Y, Qin W, Liu P, et al. An fMRI study of acupuncture using independent component analysis. Neurosci Lett 2008;449:6–9.
14. Bai L, Qin W, Tian J, et al. Time-varied characteristics of acupuncture effects in fMRI studies. Hum Brain Mapp 2009;10: 3445–3460.
15. Qin W, Tian J, Pan X, Yang L, Zhen Z. The correlated network of acupuncture effect: a functional connectivity study. Conf Proc IEEE Eng MedBiol Soc 2006;1:480–483.
16. Reijneveld JC, Ponten SC, Berendse HW, Stam CJ. The application of graph theoretical analysis to complex networks in the brain. Clin Neurophysiol 2007;118:2317–2331.
17. Achard S, Salvador R, Whitcher B, Suckling J, Bullmore E. A resilient, low-frequency, small-world human brain functional network with highly connected association cortical hubs. J Neurosci 2006;26:63–72.
18. Salvador R, Suckling J, Coleman MR, Pickard JD, Menon D, Bullmore E. Neurophysiological architecture of functional magnetic resonance images of human brain. Cereb Cortex 2005;15: 1332–1342.
19. Liu J, Liang J, Qin W, et al. Dysfunctional connectivity patterns in chronic heroin users: an fMRI study. Neurosci Lett 2009;460: 72–77.
20. Manheimer E, Lim B, Lao L, Berman B. Acupuncture for knee osteoarthritis–a randomised trial using a novel sham. Acupunct Med 2006;24:7–14.
21. Kong J, Gollub R, Huang T, et al. Acupuncture de qi, from qualitative history to quantitative measurement. J Altern Complement Med 2007;13:1059–1070.
22. Buckner RL, Sepulcre J, Talukdar T, et al. Cortical hubs revealed by intrinsic functional connectivity: mapping, assessment of stability, and relation to Alzheimer's disease. J Neurosci 2009;29: 1860–1873.
23. Harris RE, Zubieta JK, Scott DJ, Napadow V, Gracely RH, Clauw DJ. Traditional Chinese acupuncture and placebo (sham) acupuncture are differentiated by their effects on mu-opioid receptors (MORs). Neuroimage 2009;47:1077–1085.
24. Helmchen C, Mohr C, Erdmann C, Petersen D, Nitschke MF. Differential cerebellar activation related to perceived pain intensity during noxious thermal stimulation in humans: a functional magnetic resonance imaging study. Neurosci Lett 2003;335: 202–206.
25. Price DD. Psychological and neural mechanisms of the affective dimension of pain. Science 2000;288:1769–1772.
26. Treede RD, Apkarian AV, Bromm B, Greenspan JD, Lenz FA. Cortical representation of pain: functional characterization of nociceptive areas near the lateral sulcus. Pain 2000;87:113–119.
27. Mesulam MM, Mufson EJ. Insula of the old world monkey: III. Efferent cortical output and comments on function. J Comp Neurol 1982;212:38–52.
28. Casey KL. Forebrain mechanisms of nociception and pain: analysis through imaging. Proc Natl Acad Sci U S A 1999;96: 7668–7674.
29. Damasio AR, Grabowski TJ, Bechara A, et al. Subcortical and cortical brain activity during the feeling of self-generated emotions. Nat Neurosci 2000;3:1049–1056.
30. Han SH, Yoon SH, Cho YW, Kim CJ, Min BI. Inhibitory effects of electroacupuncture on stress responses evoked by tooth-pulp stimulation in rats. Physiol Behav 1999;66:217–222.
31. Manning BH, Mayer DJ. The central nucleus of the amygdala contributes to the production of morphine antinociception in the rat tail-flick test. J Neurosci 1995;15:8199–8213.
32. Mufson EJ, Mesulam MM. Insula of the old world monkey: II. Afferent cortical input and comments on the claustrum. J Comp Neurol 1982;212:23–37.
33. Napadow V, Dhond RP, Kim J, et al. Brain encoding of acupuncture sensation--coupling on-line rating with fMRI. Neuroimage 2009;47:1055–1065.